Oscillator strengths and electron collisional excitation cross sections for atomic oxygen

S. S. Tayal and Ronald J. W. Henry
Department of Physics and Astronomy, Louisiana State University, Baton Rouge, Louisiana 70803-4001
(Received 19 December 1988)

Absorption oscillator strengths for dipole-allowed transitions among the $2p^4\,^3P$, $3s\,^{5,3}S^\circ$, $3p\,^{5,3}P$, $4s\,^{5,3}S^\circ$, $3d\,^{5,3}D^\circ$, $4p\,^{5,3}P$, and $3s'\,^3D^\circ$ states of O I are calculated in length and velocity formulations using extensive configuration-interaction wave functions. We also include these 12 states in our close-coupling calculations of the inelastic cross sections for O I. Cross sections for excitation of the $3s\,^5S^\circ$, $3p\,^5P$, $4s\,^3S^\circ$, $4p\,^3P$, $3d\,^3D^\circ$, and $3s'\,^3D^\circ$ states by electron impact are presented in the energy region from 13.87 to 100 eV and these are compared, where available, with other calculations and experiments. The present results are in good agreement with the recent experiments at energies 13.87, 20, and 30 eV for the $^3P-3p\,^5P$ transition and at energies 13.87 and 16.5 eV for the $^3P-3s\,^5S^\circ$ transition. However, the present cross sections for the $^3P-3s\,^5S^\circ$ transition at 20 and 30 eV are large by a factor of 2 compared to experiment. There are discrepancies between theory and experiment in magnitude for the dipole-allowed $^3P-3d\,^3D^\circ$ and $^3P-3s'\,^3D^\circ$ transitions.

I. INTRODUCTION

In an earlier article,[1] referred to hereafter as paper I, we reported theoretical cross sections for electron-impact excitation of atomic oxygen for the electric dipole-allowed $^3P-3s\,^3S^\circ$ and -forbidden $^3P-3p\,^3P$ transitions in the energy region from 13.87 to 100 eV. The theoretical cross sections are in good agreement with the recent absolute, direct-cross-section measurements[2,3] for the resonance $^3P-3s\,^3S^\circ$ transition, while there are unresolved discrepancies between the experiment[4] and theory for the dipole-forbidden $^3P-3p\,^3P$ transition.

Excitation of the $3s\,^3S^\circ$ and $3p\,^3P$ states of atomic oxygen gives rise to prominent emission features at 1304 and 8446 Å in the spectra of the oxygen-rich atmospheres of Earth, Mars, and Venus. Some of the other prominent emission features in the spectrum of planetary atmospheres occur at 1356, 7774, 1027, and 989 Å which are associated with the excitation of the $3s\,^5S^\circ$, $3p\,^5P$, $3d\,^3D^\circ$, and $3s'\,^3D^\circ$ states of atomic oxygen, respectively. The absolute direct excitation cross sections for these transitions have recently been reported by Doering and his coworkers.[4–7] The measured relative cross sections for the excitation of the $^3P-3s\,^5S^\circ$, $^3P-3p\,^3P$, $^3P-3p\,^5P$, $^3P-3d\,^3D^\circ$, and $^3P-3s'\,^3D^\circ$ transitions in O I are placed on an absolute scale by using the known cross sections for the resonance $^3P-3s\,^3S^\circ$ transition for normalization. Stone and Zipf[8] and Zipf and Erdman[9] measured absolute electron-impact optical fluorescence cross sections for the $^3P-3s\,^3S^\circ$, $^3P-3s\,^5S^\circ$, $^3P-3d\,^3D^\circ$, and $^3P-3s'\,^3D^\circ$ transitions in O I. These measured cross sections include both direct and a number of cascade excitation contributions. Recently, Germany *et al.*[10] published absolute optical cross sections for the electron-impact excitation of the $3p\,^5P$ state of atomic oxygen in the low-energy region from 12 to 17 eV.

On the theoretical side, Julienne and Davis[11] used a distorted-wave approximation with exchange to investigate the cascade contributions from higher levels of triplet and quintet manifolds to the emission cross sections for 1304 and 1356 Å, respectively. Smith[12] and Rountree[13] performed close-coupling calculations to obtain excitation cross sections for electron-impact excitation of the resonance $^3P-3s\,^3S^\circ$ and spin-forbidden $^3P-3s\,^5S^\circ$ transitions.

In this paper we extend the work of paper I to study the electron-impact excitation of the ground ^3P state of O I to the $3s\,^5S^\circ$, $3p\,^5P$, $4s\,^3S^\circ$, $4p\,^3P$, $3d\,^3D^\circ$, and $3s'\,^3D^\circ$ states using a close-coupling approximation. In paper I the results of three independent 3-, 7-, and 12- state calculations were presented. The cross-section values differed significantly for both transitions considered in paper I in the low-energy region where strong-coupling effects among the target states play an important role, while in the high-energy region ($E > 50$ eV) the 7- and 12-state calculations gave the same results, as expected. In this paper we present the results of our best 12-state calculation. The twelve LS states $2p^4\,^3P$, $2p^3 3s\,^{5,3}S^\circ$, $2p^3 3p\,^{5,3}P$, $2p^3 4s\,^{5,3}S^\circ$, $2p^3 3d\,^{5,3}D^\circ$, $2p^3 4p\,^{5,3}P$, and $2p^3 3s'\,^3D^\circ$ are included in the close-coupling expansion. These O I states are represented by extensive configuration-interaction (CI) wave functions. For the spin-forbidden $^3P-3s\,^5S^\circ$ and $^3P-3p\,^5P$ transitions only the lower partial waves ($L = 0$–6) contribute to the cross section, while for the allowed $^3P-4s\,^3S^\circ$, $3d\,^3D^\circ$, $3s'\,^3D^\circ$ and forbidden $^3P-4p\,^3P$ transitions the higher partial waves also make significant contributions to the cross sections. Therefore, in order to obtain converged cross sections for these transitions, the lower partial-wave results obtained in the R-matrix method[14] are supplemented by higher partial-wave results calculated in a noniterative integral equation method.[15]

II. EXCITATION ENERGIES AND OSCILLATOR STRENGTHS

The wave functions are constructed with a common set of radial functions which are chosen to give the best

overall representation of the energies of the 12 states of atomic oxygen considered in the oscillator strength and scattering calculations. The CI wave function for each atomic state is represented by an expansion of the form[16]

$$\psi(LS)=\sum_{i=1}^{M} a_i\Phi_i(\alpha_i LS)\ , \tag{1}$$

where each single configuration function Φ_i is constructed from orbitals whose angular momenta are coupled, as specified by α_i, to form a total L and S common to all M configurations.

We use eight orthogonal one-electron orbitals: $1s$, $2s$, $2p$, $3s$, $3p$, $3d$, $4s$, and $4p$. The radial part of each orbital is expressed in analytic form as a sum of Slater-type orbitals and the parameters of the orbitals are obtained by optimizing the energy differences and oscillator strengths between the atomic states, as discussed in paper I. The values of the parameters of the non-Hartree-Fock radial functions are given in Table I. We used 32, 16, and 22 configurations for the description of the ^3P, $^3S^\circ$, and $^3D^\circ$ atomic-state symmetries, respectively, while 10, 13, and 6 configurations are used to describe $^5S^\circ$, ^5P, and $^5D^\circ$ atomic-state symmetries, respectively. The calculated excitation energies relative to the ground state are compared in Table II with the experiment. The agreement between the calculated and experimental energies is very good. The CI wave functions are also used to obtain absorption oscillator strengths for electric dipole-allowed transitions among the 12 O I terms. The length and velocity values of oscillator strengths are listed in Table III where they are compared with other calculations[17,18] and experiments.[19–21] Experimental values of the oscillator strengths are available for the four allowed transitions at 1304, 1040, 1027, and 989 Å given in Table III. The length and velocity values of oscillator strengths agree very well with each other, with the experiments, and with the calculation of Pradhan and Saraph[17] for the ^3P–$3s$ $^3S^\circ$, ^3P–$4s$ $^3S^\circ$, and ^3P–$3s'$ $^3D^\circ$ transitions, while for the ^3P–$3d$ $^3D^\circ$ transition the agreement is not that good. Fischer[18] reported oscillator strengths for ^3P–$3s$ $^3S^\circ$ and ^3P–$3s'$ $^3D^\circ$ transitions which are lower by about 25% than the present length values. The agreement between the length and velocity formulations and the available other calculations of Pradhan and Saraph[17] is very good for other transitions of triplet manifold considered in the present work, except for $3s$ $^3S^\circ$–$4p$ ^3P and $3p$ ^3P–$3s'$ $^3D^\circ$ transitions where oscillator strengths are small and there may be cancellations in the dipole matrix elements. The agreement between the present calculated values and the calculations of Pradhan and Saraph[17] is well within 20% for most allowed transitions between the states of quintet manifold. It should be noted that we used same nl orbitals for the representation of triplet as well as quintet states.

TABLE I. Parameters for the bound orbitals used in the calculation. Each orbital is a sum of Slater-type orbitals.

Orbital	Power of r	Exponent	Coefficient
$2p$	2	1.153 842	0.232 870
	2	1.813 985	3.057 344
	2	3.440 006	8.345 453
	2	7.577 002	3.094 479
$3s$	1	6.430 445	2.382 509
	2	2.570 288	−3.153 997
	3	0.730 919	0.142 464
$3p$	2	2.532 246	1.902 152
	3	0.511 789	−0.040 376
$3d$	3	1.602 568	0.023 741
	3	0.337 621	0.009 413
$4s$	1	6.567 021	1.093 880
	2	2.488 094	−1.377 568
	3	0.742 670	0.081 047
	4	0.393 299	−0.001 908
$4p$	2	2.525 415	1.057 326
	3	0.474 024	−0.025 104
	4	0.323 544	0.000 941

TABLE II. The calculated and experimental energies of the O I excited states relative to the ground state.

State	Energy (a.u.) Theory	Experiment[a]
$2p^4\,^3P$	0.0	0.0
$2p^3(^4S^\circ)3s\,^5S^\circ$	0.3360	0.3361
$2p^3(^4S^\circ)3s\,^3S^\circ$	0.3504	0.3499
$2p^3(^4S^\circ)3p\,^5P$	0.4012	0.3947
$2p^3(^4S^\circ)3p\,^3P$	0.4058	0.4038
$2p^3(^4S^\circ)4s\,^5S^\circ$	0.4334	0.4350
$2p^3(^4S^\circ)4s\,^3S^\circ$	0.4374	0.4384
$2p^3(^4S^\circ)3d\,^5D^\circ$	0.4434	0.4439
$2p^3(^4S^\circ)3d\,^3D^\circ$	0.4448	0.4442
$2p^3(^4S^\circ)4p\,^5P$	0.4519	0.4515
$2P^3(^4S^\circ)4p\,^3P$	0.4537	0.4542
$2p^3(^2D^\circ)3s'\,^3D^\circ$	0.4675	0.4608

[a]Reference 24.

III. DESCRIPTION OF COLLISION CALCULATIONS

The total wave function representing the scattering of electrons by O I is expanded as[22]

$$\psi_k = A\sum_{i,j} c_{ijk}\Phi_i(1,2,\ldots,8;\hat{r}_9\sigma_9)r_9^{-1}u_{ij}(r_9) + \sum_j d_{jk}\phi_j(1,2,\ldots,9)\ , \tag{2}$$

where A is the antisymmetrization operator, the Φ_i are channel functions consisting of CI wave function for the 12 atomic oxygen $2p^4\,^3P$, $2p^3 3s\,^{5,3}S^\circ$, $2p^3 3p\,^{5,3}P$, $2p^3 4s\,^{5,3}S^\circ$, $2p^3 3d\,^{5,3}D^\circ$, $2p^3 4p\,^{5,3}P$, $2p^3 3s'\,^3D^\circ$ eigenstates coupled with spin and angular functions for the scattered electron, and u_{ij} are the numerical basis functions describing the radial motion of the scattered electron. The continuum functions u_{ij} are constrained to be orthogonal to all bound orbitals. The functions ϕ_j in the second summation of Eq. (2) are of bound-state type and are included to compensate for the imposition of orthogonality conditions. Additional functions ϕ_j are included

TABLE III. Oscillator strengths for allowed transitions in O I.

Transition	Present calculation f_L	Present calculation f_V	Other theory Ref. 17	Other theory Ref.18	Experiment
$2p^4\,^3P-2p^3 3s\,^3S^\circ$	0.056	0.053	0.054	0.042	0.048,[a] 0.047,[b] 0.049[c]
$2p^4\,^3P-2p^3 4s\,^3S^\circ$	0.0098	0.0098	0.0092		0.010±0.02[a]
$2p^4\,^3P-2p^3 3d\,^3D^\circ$	0.030	0.023	0.020		0.019±0.001[a]
$2p^4\,^3P-2p^3 3s'\,^3D^\circ$	0.060	0.051	0.056	0.045	0.061±0.006[a]
$2p^3 3s\,^3S^\circ-2p^3 3p\,^3P$	1.07	1.09	1.06		
$2p^3 3s\,^3S^\circ-2p^3 4p\,^3P$	0.000 03	0.023	0.0096		
$2p^3 3p\,^3P-2p^3 4s\,^3S^\circ$	0.206	0.216	0.187		
$2p^3 3p\,^3P-2p^3 3d\,^3D^\circ$	1.01	0.933	0.966		
$2p^3 3p\,^3P-2p^3 3s'\,^3D^\circ$	0.0002	0.0001	0.0015		
$2p^3 3s\,^5S^\circ-2p^3 3p\,^5P$	1.09	0.818	0.978		
$2p^3 3s\,^5S^\circ-2p^3 4p\,^5P$	0.012	0.003	0.003		
$2p^3 3p\,^5P-2p^3 4s\,^5S^\circ$	0.137	0.177	0.164		
$2p^3 3p\,^5P-2p^3 3d\,^5D^\circ$	0.848	0.986	0.926		
$2p^3 4s\,^5S^\circ-2p^3 4p\,^5P$	1.72	1.23	1.46		
$2p^3 3d\,^5D^\circ-2p^3 4p\,^5P$	0.146	0.150	0.159		

[a]Reference 19.
[b]Reference 20.
[c]Reference 21.

to give improved accuracy. The bound configurations allow for electron correlation effects. These also may give rise to the unphysical pseudoresonances in the cross sections for electron energies above the highest excitation threshold. In order to obtain smooth cross sections in the region of pseudoresonances, we used the T-matrix smoothing procedure.[23] We calculated T matrices over the pseudoresonance regions at a fine energy mesh. The real and imaginary parts of the T matrices are then energy averaged for each partial wave.

The configuration space is partitioned into two regions. In the inner region electron exchange and correlation effects are taken into account, while in the outer region these are neglected. A boundary radius $r=46.2$ a.u. is introduced which is large compared with the mean radii of the target orbitals. The coefficients c_{ijk} and d_{jk} are determined by diagonalizing the total Hamiltonian of electron plus O I system in the basis defined by Eq. (2). We included 40 continuum orbitals in each channel, giving good convergence for energies up to 100 eV. In order to obtain converged cross sections the R-matrix results for lower partial waves ($L=0$–7) are supplemented by higher partial-wave results ($L=8$–28) obtained in the noniterative integral equation method.[15] Exchange effects are negligible for higher partial waves. In our calculation of higher partial waves, we neglected exchange, correlation, and orthogonality terms.

IV. RESULTS AND DISCUSSION

In Figs. 1–5 we show the present theoretical cross sections for the $^3P-3s\,^5S^\circ$, $^3P-3p\,^5P$, $^3P-3d\,^3D^\circ$, $^3P-3s'\,^3D^\circ$, $^3P-4s\,^3S^\circ$, and $^3P-4p\,^3P$ transitions in O I, where these are compared with the available measured values and calculations. The present results are shown by solid curves, while the measured values are displayed by solid circles.

The cross sections for the spin-forbidden $^3P-3s\,^5S^\circ$ transition are shown in Fig. 1 over the incident electron energies from 13.87 to 100 eV. In this figure we also plot the measured direct excitation cross sections of Doering and Gulcicek[7] (solid circles) and two-state close-coupling (CC) results of Smith[12] (dashed curve). The two-state CC results of Smith[12] are lower than the present results. The discrepancy in the two sets of calculations is due to the difference in the target wave functions and the number of

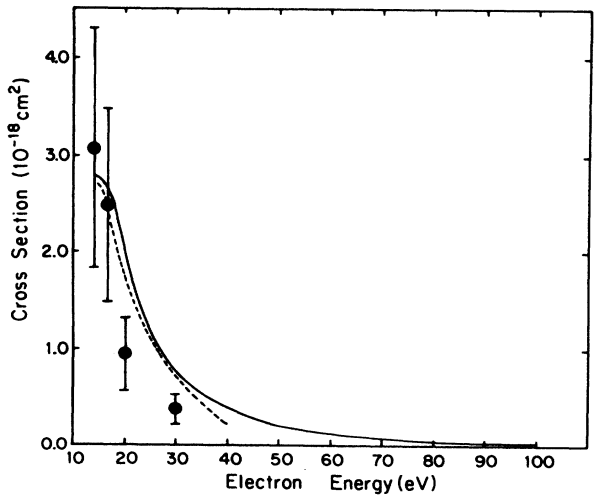

FIG. 1. Total cross sections for electron-impact excitation of the ground state to the $3s\,^5S^\circ$ state as a function of incident energy. Solid curve, 12-state CC cross sections from this work; dashed curve, two-state CC results of Smith (Ref. 12); solid circles, measured values of Doering and Gulcicek (Ref. 7).

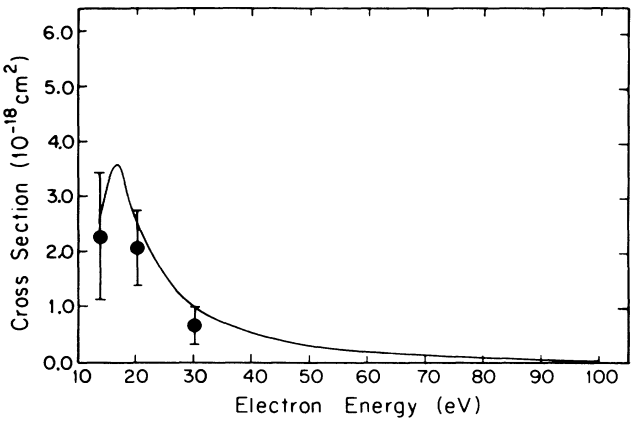

FIG. 2. Total cross sections for electron-impact excitation of the ground state to the $3p\ ^5P$ state as a function of incident energy. Notations are as in Fig. 1 except that the solid circles here represent the measured values of Gulcicek *et al.* (Ref. 4).

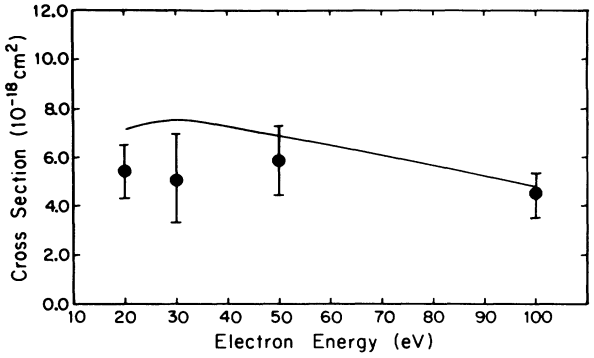

FIG. 4. Total cross sections for electron-impact excitation of the ground state to the $3s'\ ^3D^\circ$ state as a function of incident energy. Notations are as in Fig. 1 except that the solid circle at 20 eV is the measured value of Gulcicek and Doering (Ref. 2) and the solid circles at 30, 50, and 100 eV are the measured values of Vaughan and Doering (Ref. 5).

target states included in the CC expansion. The experimental results are available in 13.87–30-eV energy range. The present theoretical cross sections are well within the experimental error bars for energies 13.87 and 16.5 eV, but for energies 20 and 30 eV the theoretical cross sections are larger by a factor of 2 than the experiment. The peak value of the cross section is 2.8×10^{-18} cm^2 around 14 eV, which is in excellent agreement with the measured value of 3×10^{-18} cm^2 ($\pm40\%$). The cross sections for this transition exhibit expected falloff with increasing energy.

In Fig. 2 we display cross sections for the forbidden ^3P–$3p\ ^5P$ transition over the energy range 13.87–100 eV. We have also shown the absolute direct excitation cross sections (solid circles) of Gulcicek *et al.*[4] which are available at energies 13.87, 20, and 30 eV. The present theoretical cross sections agree with the experiment within the experimental errors at all the three energies. The cross sections show a peak around 16 eV, in agreement with the experiment of Germany *et al.*[10] The present peak value of the cross section is 3.6×10^{-18} cm^2. The emission cross sections of Germany *et al.* include cascade contributions from higher-lying quintet states in addition to the direct excitation cross section.

The present cross sections for the dipole-allowed ^3P–$3d\ ^3D^\circ$ and ^3P–$3s'\ ^3D^\circ$ transitions are plotted in Figs. 3 and 4, respectively, along with the absolute direct excitation cross sections of Vaughan and Doering[5,6] and Gulcicek and Doering.[2] The present results show significant differences with the experiments in magnitude. The theoretical cross sections for the ^3P–$3d\ ^3D^\circ$ transition show a maximum at about 25 eV, outside the range of the

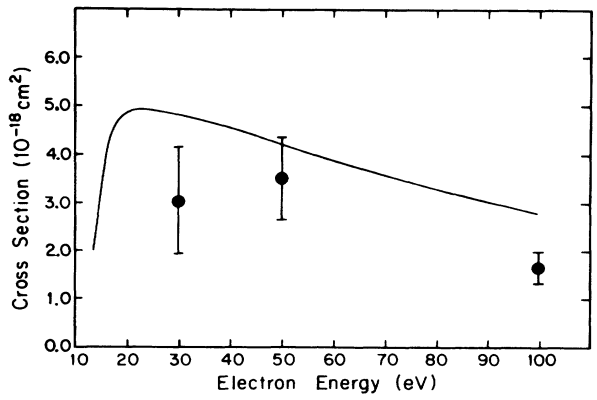

FIG. 3. Total cross sections for electron-impact excitation of the ground state to the $3d\ ^3D^\circ$ state as a function of incident energy. Notations are as in Fig. 1 except that the solid circles here represent the measured values of Vaughan and Doering (Ref. 6).

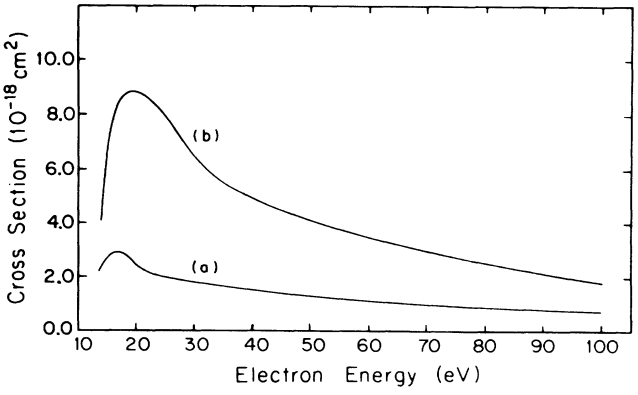

FIG. 5. Total cross sections for electron-impact excitation of the ground state to (a) $4s\ ^3S^\circ$ and (b) $4p\ ^3P$ states as a function of incident energy.

measurements. The experimental values are available at energies 30, 50, and 100 eV. The theoretical cross section lies within experimental error bar at 50 eV, while at 30 and 100 eV the present cross sections are larger than the experiment by about a factor of 1.5. The use of approximate wave functions may be the cause of this discrepancy for the ^3P–$3d\ ^3D^\circ$ transition where the calculated length value of the oscillator strength is larger by about 50% than the measured value. The direct excitation cross sections of Vaughan and Doering[6] are in agreement with the emission cross section of Zipf and Erdman[9] (not shown) within the experimental error at 30 and 50 eV (see Fig. 3 of the paper of Vaughn and Doering[6]). It should be noted that the emission cross sections of Zipf and Erdman[9] represent the sum of $3d\ ^3D^\circ$ direct excitation and the cascade contributions from higher-lying triplet states.

The theoretical cross sections for the dipole-allowed ^3P–$3s'\ ^3D^\circ$ transition (Fig. 4) agree with the measured direct excitation cross sections of Vaughan and Doering[5] within the experimental errors at 50 and 100 eV, but at lower energies (20 and 30 eV) the present cross sections are larger than the experiment. The measured values of Vaughan and Doering[5] were recently revised at 20 eV by Gulcicek and Doering[2] because they remeasured the cross sections for the ^3P–$3s\ ^3S^\circ$ transition in the low-energy region ($E < 30$ eV). The cross sections for the resonance ^3P–$3s\ ^3S^\circ$ transition are being used as a reference cross section for the normalization of the cross sections for other transitions. The revised value at 20 eV for the ^3P–$3s'\ ^3D^\circ$ transition is larger than the previous value by a factor of 2. The emission cross sections of Zipf and Erdman[9] (not shown) are two to three times larger than the direct excitation cross sections for this transition. Vaughan and Doering[5] have indicated that the emission cross sections may remain larger by a factor of 2 compared to their direct excitation cross sections even after subtracting the cascade contributions. We include 12 O I states with $3s'\ ^3D^\circ$ being the highest-excited state included in the CC expansion. In other words, we ignored the coupling of this state with higher-lying states of ^3F, ^3D, and ^3P symmetries which may be important. For this reason, the present results for ^3P–$3s'\ ^3D^\circ$ transition may be in error. The pseudoresonances may be the other source of some error in the present cross sections in the energy region between 15 and 30 eV. The cross sections for several partial waves contained pseudoresonances in the energy region $15 \leq E \leq 30$ eV which are smoothed over using the T-matrix-smoothing procedure.[23] For ^3P–$3s'\ ^3D^\circ$ transition we encountered pseudoresonances just above the excitation threshold and extending to about 28 eV which produced some problems in the lower-energy region. Therefore, we omitted our low-energy results ($E < 20$ eV) for ^3P–$3s'\ ^3D^\circ$ transition.

In Fig. 5 we display our theoretical cross sections for the ^3P–$4s\ ^3S^\circ$ and ^3P–$4p\ ^3P$ transitions by solid curves 5(a) and 5(b), respectively. The peak value of the cross section for ^3P–$4s\ ^3S^\circ$ transition is 2.9×10^{-18} cm^2 at about 17 eV, while for ^3P–$4p\ ^3P$ transition it is 8.8×10^{-18} cm^2 and occurs at about 20 eV, and the cross sections for both transitions then decrease with increasing energy. The allowed transition is weaker than the forbidden transition. In paper I we noticed that the magnitude of the cross sections for the dipole-allowed ^3P–$3s\ ^3S^\circ$ and -forbidden ^3P–$3p\ ^3P$ transitions were comparable for energies $E < 50$ eV which we attributed to the presence of strong indirect couplings. A similar situation seems to exist for the $4p\ ^3P$ state which is being populated by intermediate states.

In conclusion, we presented theoretical cross sections for electron-impact excitation of the ^3P–$3s\ ^5S^\circ$, ^3P–$3p\ ^5P$, ^3P–$4s\ ^3S^\circ$, ^3P–$3d\ ^3D^\circ$, ^3P–$4p\ ^3P$, and ^3P–$3s'\ ^3D^\circ$ transitions in O I which give rise to prominent emission features in the dayglow and aurora. The theoretical cross sections for the excitation of the $3s\ ^5S^\circ$ and $3p\ ^5P$ states are normally in good agreement with the experiment and display the characteristic shape of the spin-forbidden transitions, but for the dipole-allowed ^3P–$3d\ ^3D^\circ$ and ^3P–$3s'\ ^3D^\circ$ transitions there are discrepancies in magnitude. Truncation of the close-coupling expansion to 12 low-lying states and smoothening of the pseudoresonances may introduce some errors in the present results in the low-energy region ($E < 30$ eV). However, we believe our results to be quite accurate and reliable for energies $E \geq 30$ eV.

ACKNOWLEDGMENTS

This research was supported in part by National Aeronautics and Space Administration Grant No. NAGW-48.

[1]S. S. Tayal and R. J. W. Henry, Phys. Rev. A **38**, 5945 (1988).
[2]E. E. Gulcicek and J. P. Doering, J. Geophys. Res. **93**, 5879 (1988).
[3]S. O. Vaughan and J. P. Doering, J. Geophys. Res. **91**, 13 755 (1986).
[4]E. E. Gulcicek, J. P. Doering, and S. O. Vaughan, J. Geophys. Res. **93**, 5885 (1988).
[5]S. P. Vaughan and J. P. Doering, J. Geophys. Res. **92**, 7749 (1988).
[6]S. O. Vaughan and J. P. Doering, J. Geophys. Res. **92**, 289 (1988).
[7]J. P. Doering and E. E. Gulcicek, J. Geophys. Res. (to be published).
[8]E. J. Stone and E. C. Zipf, J. Chem. Phys. **60**, 4237 (1974).
[9]E. C. Zipf and P. W. Erdman, J. Geophys. Res. **90**, 11 087 (1985).
[10]G. A. Germany, R. J. Anderson, and G. F. Salamo, J. Chem. Phys. **89**, 1999 (1988).
[11]P. S. Julienne and J. Davis, J. Geophys. Res. **81**, 1397 (1976).
[12]E. R. Smith, Phys. Rev. A **13**, 65 (1976).
[13]S. P. Rountree, J. Phys. B **10**, 2719 (1977).
[14]K. A. Berrington, P. G. Burke, M. Le Dourneuf, W. D. Robb,

K. T. Taylor, and Vo Ky Lan, Comput. Phys. Commun. **14**, 367 (1978).
[15]R. J. W. Henry, S. P. Rountree, and E. R. Smith, Comput. Phys. Commun. **23**, 233 (1981).
[16]A. Hibbert, Comput. Phys. Commun. **9**, 141 (1975).
[17]A. K. Pradhan and H. E. Saraph, J. Phys. B **10**, 3365 (1977).
[18]C. F. Fischer, J. Phys. B **20**, 1193 (1987).
[19]J. P. Doering, E. E. Gulcicek, and S. O. Vaughan, J. Geophys. Res. **90**, 5279 (1985).
[20]G. M. Lawrence, Phys. Rev. A **2**, 397 (1970).
[21]W. R. Ott, Phys. Rev. A **4**, 245 (1971).
[22]P. G. Burke, A. Hibbert, and W. D. Robb, J. Phys. B **4**, 153 (1971).
[23]P. G. Burke, K. A. Berrington, and C. V. Sukumar, J. Phys. B **14**, 289 (1981).
[24]C. E. Moore, *Atomic Energy Levels,* Natl. Bur. Stand. Ref. Data Ser., Natl. Bur. Stand. (U.S.) Circ. No. 35 (U.S. GPO, Washington, D.C., 1971), Vol. 1.